Title
Absorption and scattering by long and randomly oriented linear chains of spheres

Journal
Journal of the Optical Society of America A, 30(9)

ISSN
1084-7529 1520-8532

Authors
Lee, Euntaek
Pilon, Laurent

Publication Date
2013-08-30

DOI
10.1364/JOSAA.30.001892

Peer reviewed

Absorption and Scattering by Long and Randomly Oriented Linear Chains of Spheres

Euntaek Lee and Laurent Pilon

Mechanical and Aerospace Engineering Department
Henry Samueli School of Engineering and Applied Science
University of California, Los Angeles - Los Angeles, CA 90095, USA
Phone: +1 (310)-206-5598, Fax: +1 (310)-206-2302
E-mail: pilon@seas.ucla.edu

E. Lee, and L. Pilon, 2013. "Absorption and Scattering by Long and Randomly Oriented Linear Chains of Spheres", *Journal of the Optical Society of America A*, Vol. 30, pp. 1892-1900. doi:/10.1364/JOSAA.30.001892

Abstract

This paper demonstrates that the scattering cross-section per unit length of randomly oriented linear chains of monodisperse spheres asymptotically converges towards those of randomly oriented and infinitely long cylinders with volume-equivalent diameter as the number of spheres increases. The critical number of spheres necessary to approximate the linear chains of spheres as infinitely long cylinders decreased rapidly as the size parameter of an individual sphere increased from 0.01 to 10. On the other hand, their absorption cross-section per unit length was identical to that of infinitely long volume-equivalent cylinder for any number of spheres. However, this approximation does not apply to the angle-dependent Stokes scattering matrix element ratios.

1 Introduction

Light absorption and scattering by non-spherical particles or by clusters of spheres has been a subject of great interest in the radiation transfer community and has found various applications in science and engineering ranging from astrophysics and atmospheric science to combustion systems and aerosol-based processes [1–4]. Numerical tools have been developed to predict light absorption and scattering by non-spherical scatterers based on (i) the T-matrix method [5–9], (ii) the discrete-dipole approximation (DDA) [10–12], or (iii) the finite-difference time-domain method [3, 13, 14], to name the most widely used. Similarly, light absorption and scattering by a cluster or aggregate of spheres has been predicted by (i) the superposition T-matrix method [15–21], (ii) the DDA [22], and (iii) by the volume-integral equation formulation combined with the method of moments [23–25]. Most of the studies on sphere clusters focused on radiation scattering and absorption by soot particles.

Depending on the size and morphology of the scatterers and on the wavelength, calculations can be time consuming and require large computing resources regardless of the method used. Thus, for practical purposes, it is important to try to find simplified models to approximate scatterers with complex geometries as equivalent particles with simpler shapes such

as spheres or cylinders [14, 26]. For example, Kahnert *et al.* [26] showed that the extinction and scattering cross-sections, the single scattering albedo, and the asymmetry factor of an ensemble of randomly oriented polyhedral prisms with power-law size distribution and size comparable to the wavelength of light can be approximated as an ensemble of spheres, spheroids, or finite-length cylinders with the same volume, complex index of refraction, and size distribution. Note that treating the prisms as volume-equivalent cylinders or spheroids gave slightly better results than treating them as spheres. However, any of these simplifications failed to predict the linear depolarization ratio. Similarly, Yang *et al.* [14] investigated the single scattering properties of various Platonic particles and compared their radiation characteristics with those of equivalent spheres having the same (i) geometric dimension, (ii) surface area, (iii) volume, or (iv) volume to surface area ratio. The authors concluded that all these approximations led to significant errors in the extinction efficiency factor, single scattering, albedo, and/or scattering matrix elements. The volume-equivalent spheres gave the smallest errors of all equivalent spheres considered. In addition, approximating the Platonic particles by their volume to surface area ratio equivalent sphere led to the largest errors.

The goal of the present study is to theoretically identify simplified models for predicting light absorption and scattering by long and randomly oriented linear chains of spheres. This question finds its motivation in predicting light transfer in photobioreactors cultivating photosynthetic filamentous cyanobacteria for wastewater treatment, sustainable biofuel, and/or fertilizer productions. It also applies to the field of ocean optics for remote sensing applications and for studying carbon dioxide and nitrogen cycles [4], for example.

2 Background

2.1 Filamentous Cyanobacteria

Cyanobacteria, also known as blue-green algae, are photo-autotrophic prokaryotes that are capable of conducting oxygenic photosynthesis [27]. They use solar radiation in the photosynthetically active radiation (PAR) region, defined by wavelength ranging from 400 to 700 nm, as their energy source. They can be found in nearly every terrestrial and aquatic habitat on Earth and are responsible for the presence of oxygen in the atmosphere [28]. Cyanobacteria can be unicellular and filamentous and their size can range from 0.5 μm to 40 μm in diameter depending on the strain [27]. Some filamentous forms have evolved to contain the nitrogenase enzyme in specialized nitrogen-fixing cells called heterocysts. Several species can also produce hydrogen H_2 through direct and indirect biophotolysis and have been considered for photobiological hydrogen production [29].

Figure 1 shows micrographs of different species of filamentous cyanobacteria and illustrates, in particular, (a) nearly spherical vegetative cells of the nitrogen-fixing cyanobacteria *Nostoc punctiforme* 5-6 μm in diameter, (b) an ensemble of *Nostoc punctiforme* showing filaments with both vegetative (5-6 μm in diameter) and heterocyst cells (6-10 μm in diameter), (c) individual filament of *Anaebena sp.* with spherical to oblong vegetative cells 4-14 μm in diameter, and (d) aggregating filaments of *Anabaena iyengari*. Other filamentous cyanobacteria with similar morphology include *Anabaena sphaerica*, *Anabaena cylindrica*,

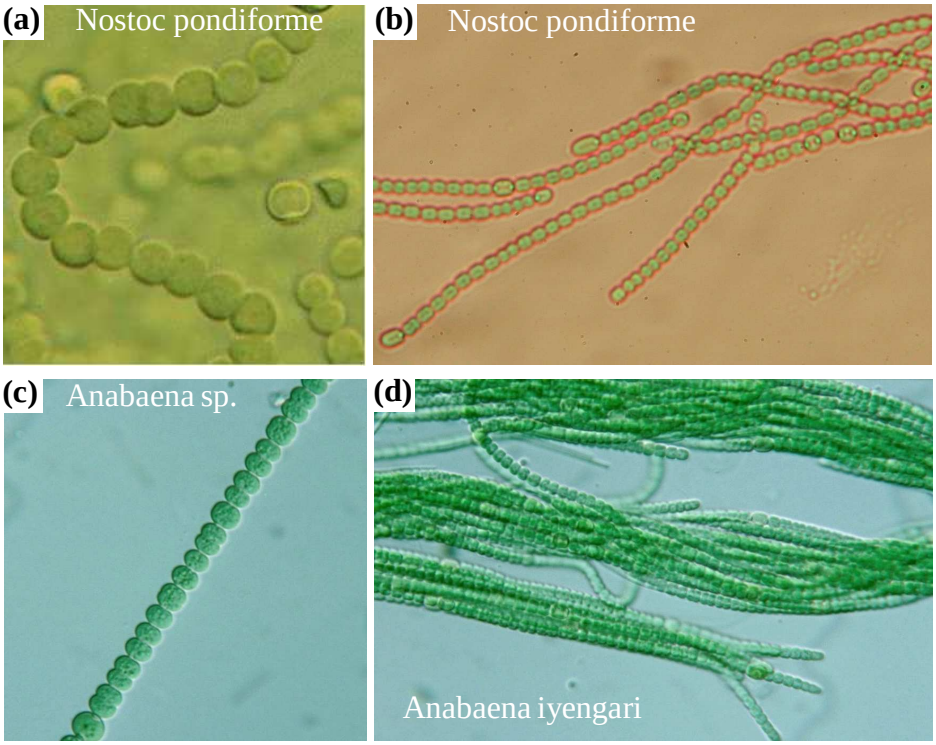

Figure 1: Micrographs of filamentous cyanobacteria (a) and (b) *Nostoc pondiforme*, (c) *Anabaena sp.*, and (d) *Anabaena iyengari*. Image credit, reproduced with permission from: (a) Isao Inouye (University of Tsukuba). Mark Schneegurt (Wichita State University), and Cyanosite (www-cyanosite.bio.purdue.edu), (b) Prof. Ann Magnuson (Uppsala University), (c) and (d) Prof. Yuuji Tsukii (Hosei University, http://protist.i.hosei.ac.jp/)

Anabaena variabilis, and *Anabaena azollae*, to name a few.

2.2 Scattering Matrix

The radiation incident on a particle of arbitrary shape at location $\mathbf{r}$ can be represented by the incident Stokes vector $\mathbf{I}_{inc}(\mathbf{r}, \hat{s}_i) = (I_{inc}, Q_{inc}, U_{inc}, V_{inc})^T$ where I, Q, U, and V are the so-called Stokes parameters [30]. The Stokes vector of the scattered radiation denoted by $\mathbf{I}_{sca}(\mathbf{r}, \hat{s}) = (I_{sca}, Q_{sca}, U_{sca}, V_{sca})^T$ is related to the incident Stokes vector by the Mueller scattering matrix $[\mathbf{Z}(\Theta)]$ according to [17],

$$\mathbf{I}_{sca}(\mathbf{r}, \hat{s}) = \frac{1}{r^2}[\mathbf{Z}(\Theta)]\mathbf{I}_{inc}(\mathbf{r}, \hat{s}_i) \tag{1}$$

where r is the norm of the location vector $\mathbf{r}$ and Θ is the so-called scattering angle ranging from 0 to 180^o and defined as the angle between the incident and scattered directions denoted by $\hat{s}_i$ and $\hat{s}$, respectively. For a cluster of particles with a plane of symmetry, it is convenient to use the reduced (or Stokes) scattering matrix expressed as [17]

$$[\mathbf{F}(\Theta)] = \frac{4\pi}{C_{sca}}[\mathbf{Z}(\Theta)] \tag{2}$$

where C_{sca} is the particle's scattering cross-section. Then, the reduced scattering matrix has a 4×4 structure with 6 independent elements and can be written as [2],

$$[\mathbf{F}(\Theta)] = \begin{bmatrix} F_{11}(\Theta) & F_{12}(\Theta) & 0 & 0 \\ F_{12}(\Theta) & F_{22}(\Theta) & 0 & 0 \\ 0 & 0 & F_{33}(\Theta) & F_{34}(\Theta) \\ 0 & 0 & -F_{34}(\Theta) & F_{44}(\Theta) \end{bmatrix} \tag{3}$$

The reduced scattering matrix element $F_{11}(\Theta)$ is the scattering phase function normalized according to

$$\frac{1}{4\pi} \int_{4\pi} F_{11}(\Theta) \sin\Theta d\Theta = 1 \tag{4}$$

In addition, the first moment of the scattering phase function is the so-called asymmetry factor defined as [31]

$$g = \int_{4\pi} F_{11}(\Theta) \cos\Theta d\Omega \tag{5}$$

It describes the shape of the scattering phase function and is equal to 0.0 for isotropic scattering and -1 and 1 for purely backward and forward scattering, respectively.

The ratio $-F_{12}(\Theta)/F_{11}(\Theta)$ represents the degree of linear polarization of the scattered radiation for unpolarized incident radiation [32]. The ratio $F_{22}(\Theta)/F_{11}(\Theta)$ captures the non-sphericity of the particles and is equal to unity for a single sphere [32]. Other indicators of the sphericity of the scatterer are the linear and circular polarization ratios respectively defined as [17]

$$\delta_L = \frac{[F_{11}(180^o) - F_{22}(180^o)]}{[F_{11}(180^o) + F_{22}(180^o)]} \tag{6}$$

$$\text{and} \quad \delta_C = \frac{[F_{11}(180^o) - F_{44}(180^o)]}{[F_{11}(180^o) + F_{44}(180^o)]} \tag{7}$$

For a single sphere $\delta_{C,s} = \delta_{L,s}$ [17] while for randomly oriented rotationally symmetric particles $\delta_C \geq 2\delta_L$ [6]. For a randomly oriented and infinitely long cylinder, they both vanish, i.e., $\delta_{C,c} = \delta_{L,c} = 0$. The term F_{34} represents how much incident radiation obliquely polarized at 45^o gets transformed into circularly polarized radiation [32]. Hovenier and Mackowski [33] derived relations between scattering matrix elements at forward and backward scattering directions ($\Theta = 0$ and 180^o) for randomly oriented single particle and a cluster of particles with one plane of symmetry and for rotationally symmetric particles. They showed that, for such particles or clusters, $\Delta(0^0) = F_{11}(0) - F_{22}(0) - F_{33}(0) + F_{44}(0)$ was equal to zero and that $F_{11}(180^o) - 2F_{22}(180^o) = F_{44}(180^o)$. These relationships were validated using the T-matrix method. Finally, for a spherical scatterer $F_{22}(\Theta) = F_{11}(\Theta)$ and $F_{33}(\Theta) = F_{44}(\Theta)$ [30].

2.3 T-matrix Method for Linear Chain of Spheres

The superposition T-matrix method has been developed for arbitrary clusters of multiple spheres as described in details in Ref. [16]. This approach is based on the superposition

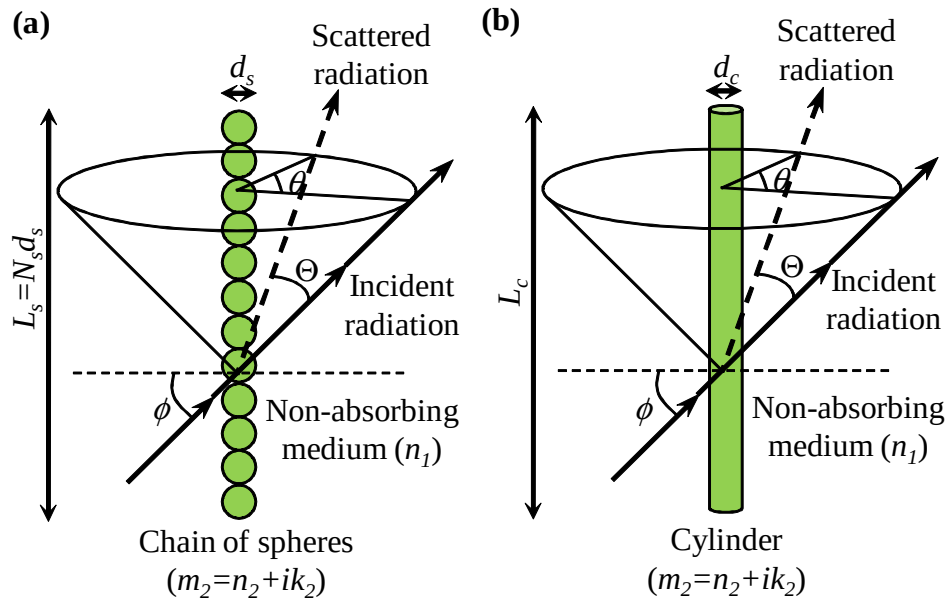

Figure 2: Schematic and coordinate system associated with absorption and scattering of incident radiation at incident angle of ϕ by (a) a linear chain of N_s spheres of diameter d_s with complex index of refraction $m_2 = n_2 + ik_2$ in a non-absorbing medium of $m_1 = n_1$ and (b) an infinitely long cylinder of diameter d_c [34].

principles whereby the scattered field from the entire cluster of spheres is estimated by summing those from each of the spheres [16]. The scattered fields in sphere-centered coordinate are also transformed into cluster-centered coordinates [16]. The absorption and scattering cross-sections and efficiency factors for randomly oriented clusters of identical spheres can be obtained by using the matrix relationships for the scattered and incident field and integrating the incident field over all propagation directions and polarizations [21]. The corresponding Stokes scattering matrix can be obtained analytically from operations on the T-matrix [21].

Figure 2a illustrates absorption and scattering by a linear chain of monodisperse spheres of complex index of refraction $m_2 = n_2+ik_2$ in a non-absorbing medium of refraction index n_1. Mackowski and Mishchenko [21] defined the orientation-averaged absorption and scattering cross-sections of a cluster of N_s monodisperse spheres, denoted by $\langle C_{abs,s}\rangle\,(m, \chi_s, N_s)$ and $\langle C_{sca,s}\rangle\,(m, \chi_s, N_s)$, respectively and expressed in m^2, as

$$\left\langle C_{abs/sca,s}\right\rangle = \frac{\pi d_{s,eq,V}^2}{4}\left\langle Q_{abs/sca,s}\right\rangle \tag{8}$$

where $d_{s,eq,V}$ is the equivalent diameter of a single sphere having volume identical to that of the cluster of N_s monodisperse spheres of diameter d_s, i.e., $d_{s,eq,V} = d_s N_s^{1/3}$. Here, $m = m_2/n_1$ is the relative complex index of refraction of the cylinder with respect to that of the non-absorbing surrounding medium while $\chi_s = \pi d_s/\lambda$ is the size parameter of a single sphere of diameter d_s. The notation $\langle X\rangle$ refers to the orientationally averaged property. The absorption and scattering efficiency factors denoted by $\langle Q_{abs,s}\rangle(m, \chi_s, N_s)$ and $\langle C_{sca,s}\rangle(m, \chi_s, N_s)$ were computed by the T-matrix method.

Numerous studies have been concerned with light absorption and scattering by fractal aggregates of small spherical particles simulating soot particles forming in combustion systems [20, 23–25, 35]. Mischchenko and Mackowski [15] demonstrated the use of the T-matrix method to determine the elements of the Stokes scattering matrix for randomly oriented and connected bispheres. The authors extended this formulation to determine the elements of the scattering matrix of randomly oriented arbitrary clusters of spheres [19]. In particular, they considered linear chains of spheres consisting of 1 to 5 spheres with size parameter χ_s= 5 and relative complex index of refraction m = 1.5 + i 0.005 [19]. They concluded that increasing the number of spheres (i) enhanced scattering in the forward direction ($\Theta = 0\ ^o$) and (ii) damped out the oscillations in the Stokes scattering matrix elements as a function of scattering angle Θ. In addition, the elements F_{11}, F_{12}, F_{22}, F_{33}, F_{34}, and F_{44} became nearly independent of the number of spheres for chains consisting of two spheres or more. To illustrate their symmetry relations for forward and backward scattering by randomly oriented clusters of spheres with a plane of symmetry, Hovenier and Mackowski [33] considered a linear chain of spheres consisting of 4 spheres with size parameter χ_s= 3 and relative complex index of refraction m = 1.311 + i 3.11$\times\ 10^{-9}$ and showed that $\Delta(0^o) = 0$ [19].

2.4 Lorenz-Mie Theory for Infinitely Long Cylinders

Figure 2b illustrates absorption and scattering by an infinitely long cylinder of diameter d_c with complex index of refraction $m_2 = n_2 + ik_2$ in a non-absorbing medium of refraction index n_1. Collimated radiation is incident onto the cylinder at an angle ϕ with respect to the normal of the cylinder axis [34]. The scattered radiation propagates along the conical surface defined by the apex angle of $\pi/2 - \phi$. The direction of the scattered radiation is defined azimuthally relative to the incident radiation by the angle θ. The Lorenz-Mie theory predicting the absorption and scattering cross-sections of infinitely long cylinders is well established [1, 2, 34, 36–39]. First, cylinders can be treated as infinitely long provided that their length L_c is much larger than their diameter d_c, i.e., $L_c \gg d_c$ [2]. The extinction and scattering cross-sections per unit length of an infinitely long cylinder of diameter d_c with relative complex index of refraction m for a given incident direction ϕ are denoted by $C'_{ext,c}$ and $C'_{sca,c}$ and expressed in m^2/m. They are defined as [40]

$$C'_{ext/sca,c}(m, \chi_c, \phi) = 2d_c Q_{ext/sca,c}(m, \chi_c, \phi) \tag{9}$$

where $\chi_c = \pi d_c/\lambda$ is the cylinder size parameter while $Q_{ext,c}(m, \chi_c, \phi)$ and $Q_{sca,c}(m, \chi_c, \phi)$ are the extinction and scattering efficiency factors, respectively. The extinction and scattering cross-sections $C'_{ext,c}(m, \chi_c, \phi)$ and $C'_{sca,c}(m, \chi_c, \phi)$ can be expressed in terms of the Lorenz-Mie scattering coefficients a_n and b_n given in terms of Bessel and Hankel functions [1, 40]. In addition, the absorption cross-sections per unit length is defined as $\left\langle C'_{abs,c}\right\rangle (m, \chi_c) = \left\langle C'_{ext,c}\right\rangle (m, \chi_c) - \left\langle C'_{sca,c}\right\rangle (m, \chi_c)$ The absorption and scattering cross-sections per unit length of an infinitely long and randomly oriented cylinder is estimated by averaging the angular cross-sections over the observation hemisphere according to [34]

$$\left\langle C'_{abs/sca,c}\right\rangle (m, \chi_c) = \int_0^{\pi/2} C'_{abs/sca,c}(m, \chi_c, \phi)\cos\phi \mathrm{d}\phi \tag{10}$$

where the subscript "i" refers to extinction or scattering cross-sections.

To the best of our knowledge, only a few studies have presented the Stokes scattering matrix elements of linear chains of spheres [19, 33, 41]. In addition, the number of spheres considered did not exceed 5 and a single relatively large size parameter was investigated. By contrast, the present study investigates the effect of the sphere size parameter (ranging from 0.01 to 10) and the number of spheres (between 1 and 4000) on the absorption and scattering scattering cross-sections per unit length, the scattering phase function, and the Stokes scattering matrix elements of linear chains of spheres. It aims to answer the following questions: (1) Can one approximate long and randomly oriented linear chains of spheres as randomly oriented infinitely long cylinders? (2) If so, how long should the chains be or how many spheres should it consist of? and (3) What should the diameter of the equivalent cylinder be?

3 Analysis

3.1 Problem statement

Radiation characteristics of photosynthetic microorganisms depend largely on their size, shape, pigment composition, internal structure, and effective optical properties [42]. They are essential in predicting light transfer in photobioreactors and the overall performance of the systems [31, 43, 44]. The circularity and aspect ratio of individual cells in cyanobacteria filaments are not exactly unity as suggested by micrographs shown in Figure 1. However, the average aspect ratio of vegetative or heterocyst cells is typically less than 1.33. Our previous study showed that the radiation characteristics of randomly oriented spheroidal microalgae with aspect ratio less than 1.33 computed with the T-matrix method were nearly identical to those of surface-equivalent spheres with identical complex index of refraction computed by Lorenz-Mie theory [45]. These observations suggest that, as a first order approximation, filamentous cyanobacteria can be approximated as linear chains of connected, spherical, and homogeneous cells. In a well-mixed suspension, they could further be treated as randomly oriented.

Transport of unpolarized light through well-mixed suspensions of linear chain of spheres of known concentration is governed by the radiation transfer equation requiring knowledge of their absorption and scattering cross-sections $\langle C'_{abs,\lambda} \rangle$ and $\langle C'_{sca,\lambda} \rangle$, and of the scattering phase function $F_{11}(\Theta)$. Moreover, investigating other elements of the scattering matrix could prove useful for remote sensing of these suspensions. Then, their radiation characteristics could be numerically predicted by the superposition T-matrix method [21]. However, these calculations can be very time consuming particularly given the length and size of these microorganisms and the wavelength of light in the PAR region. Therefore, from a radiation standpoint, one may wonder if these microorganisms could be modeled as randomly oriented and infinitely long cylinders [2, 34, 38].

3.2 Methodology

The computer code for the superposition T-matrix method used to predict absorption and scattering cross-sections ans Stokes scattering matrix elements of randomly oriented linear chains of monodisperse spheres was obtained from Ref. [21]. It was successfully validated by comparing predictions of the absorption and scattering efficiency factors and the Stokes scattering matrix elements predicted by our code with those (i) for randomly oriented bi-spheres with m = 1.5+i0.005 and χ_s=10 reported by Mishchenko and Mackowski [18] and (ii) for randomly oriented linear chains of spheres composed of 1 to 5 touching spheres with m = 1.5+i0.005 and χ_s=5 reported by Mackowski and Mishchenko [19]. Similarly, Lorenz-Mie theory code for randomly oriented and infinitely long cylinders used in this study was obtained from Ref. [39]. It was successfully validated against results reported by Lee [34,46] for the extinction efficiency factor and the scattering phase function of randomly oriented and infinitely long cylinder in vacuum.

Yang *et al.* [14] warned that it could be "misleading" to compare the efficiency factors of particles with complex shape with those of their equivalent spheres rather than directly comparing their cross-sections. Indeed, radiation transfer calculations use cross-sections and the particle number density N_T (in $\#/\mathrm{m}^3$) to estimate the absorption and scattering coefficients as $\kappa_\lambda = C_{abs,\lambda} N_T$ and $\sigma_{s,\lambda} = C_{sca,\lambda} N_T$. These coefficients are used to compute the radiation intensity solution of the radiative transfer equation [40]. Thus, the present study compares the absorption and scattering cross-sections of randomly oriented linear chain of spheres and infinitely long cylinders. In order to directly compare the radiation cross-sections of a randomly oriented linear chain composed of N_s spheres of diameter d_s with those of an infinitely long cylinder, their orientationally-averaged scattering and absorption cross-sections were defined per unit length of linear chain of spheres as

$$\left\langle C'_{abs/sca,s} \right\rangle = \frac{\left\langle C_{abs/sca,s} \right\rangle}{N_s d_s} \tag{11}$$

Finally, in the present study, the complex index of refraction of the spheres was taken as $m_2 = 1.355 + i0.004$ while that of the non-absorbing surrounding medium was $n_1 = 1.333$. These optical properties were representative of cyanobacteria in suspension in their nutrient medium and exposed to visible light [45]. Qualitative conclusions obtained with these properties are expected to be valid for other values of complex index of refraction even though the actual values of the cross-sections and Stokes scattering matrix elements may be different.

4 RESULTS AND DISCUSSION

4.1 Absorption and Scattering Cross-Sections

Figure 3 shows the absorption cross-section per unit length of a randomly oriented linear chain of monodisperse spheres as a function of the number of spheres N_s for size parameter χ_s= 0.01, 0.1, 1, and 10. The results were compared with those for an infinitely long cylinder with identical relative complex index of refraction. Two equivalent diameters were considered assuming (1) the cylinder had the same surface area as the chain of spheres resulting in the

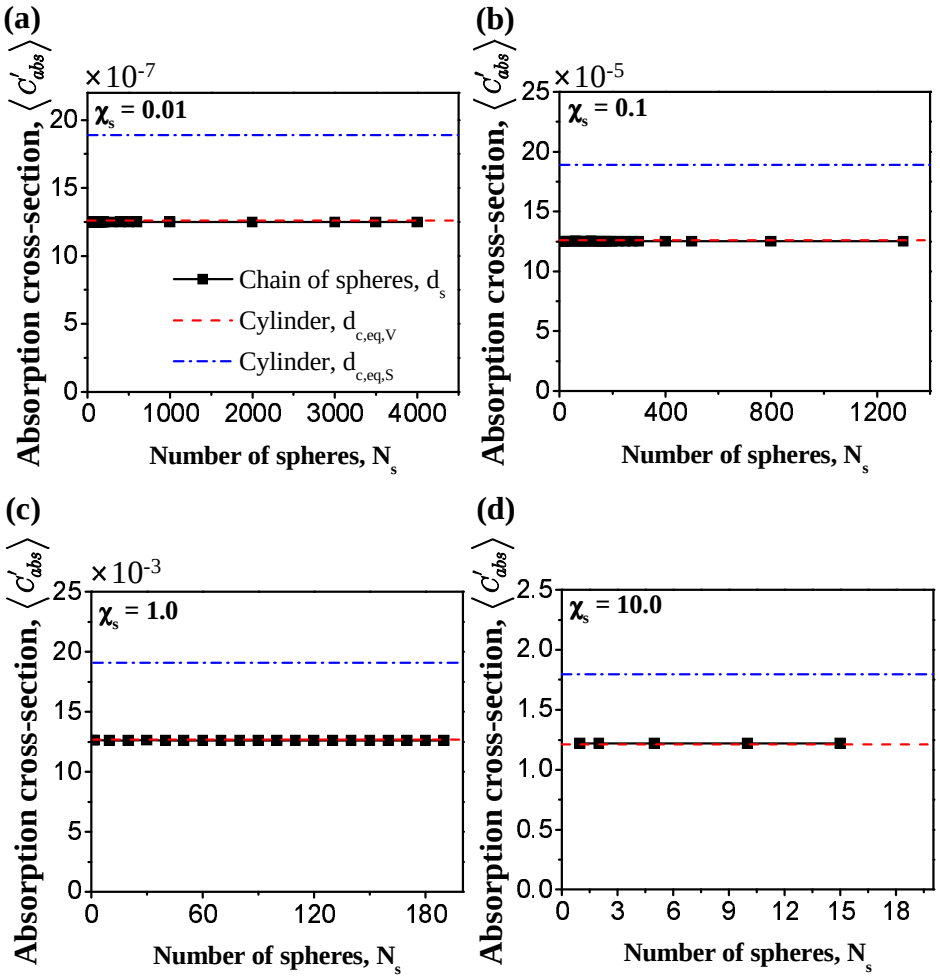

Figure 3: Absorption cross-section $\langle C'_{abs} \rangle (m, \chi_s)$ per unit length (in m) for randomly oriented linear chains of monodisperse spheres as a function of the number of spheres N_s and for randomly oriented and infinitely long equivalent cylinders of diameter $d_{c,eq,S}$ and $d_{c,eq,V}$ for size parameter χ_s=0.01, 0.1, 1.0, and 10.0 and $m = 1.0165 + i0.003$.

surface-equivalent diameter $d_{c,eq,S} = d_s$ or (2) the cylinder had the same volume as the chain of spheres resulting in volume-equivalent diameter $d_{c,eq,V} = \sqrt{2/3} d_s$. Figure 3 indicates that the absorption cross-sections per unit length of randomly oriented linear chain of spheres was equal to that of a randomly oriented and infinitely long cylinders with volume-equivalent diameter regardless of the number of spheres, i.e., $\langle C'_{abs,s} \rangle (m, \chi_s, N_s) = \langle C'_{abs,c} \rangle (m, \chi_{c,eq,V})$. However, it was much smaller than that of a randomly oriented and infinitely long cylinder with surface-equivalent diameter $d_{c,eq,S}$.

Similarly, Figure 4 shows the scattering cross-section per unit length of randomly oriented linear chain of spheres as a function of the number of spheres N_s. Four size parameters were considered namely χ_s = 0.01, 0.1, 1, and 10. These results were compared with the scattering cross-section per unit length of a randomly oriented and infinitely long cylinder with the same relative complex index of refraction m. Figure 4 indicates that the scattering

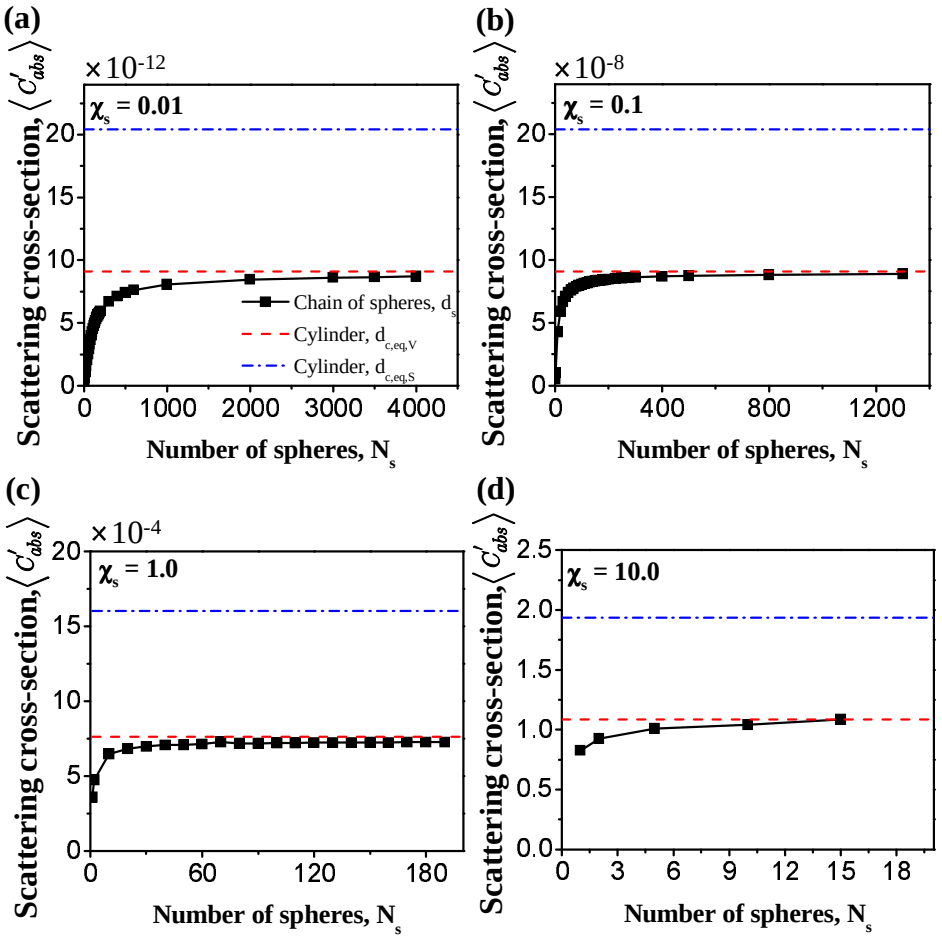

Figure 4: Scattering cross-section $\langle C'_{sca} \rangle (m, \chi_s)$ per unit length (in m^2/m) for randomly oriented linear chains of monodisperse spheres as a function of the number of spheres N_s and for randomly oriented and infinitely long equivalent cylinders of diameter $d_{c,eq,S}$ and $d_{c,eq,V}$ for size parameter χ_s=0.01, 0.1, 1.0, and 10.0 and $m = 1.0165 + i0.003$.

cross-section of linear chains of spheres increased with increasing number of spheres for all size parameters considered. In addition, as the number of spheres increased, the scattering cross-section asymptotically converged towards that of randomly oriented and infinitely long volume-equivalent cylinders with diameter $d_{c,eq,V}$.

Let us define the critical number of spheres $N_{s,cr}$ necessary to achieve an error less than 5% between the scattering cross-sections of a linear chain of spheres and those of infinitely long cylinders.

Figure 5 plots the critical number of spheres $N_{s,cr}$ as a function of size parameter χ_s. It is evident that $N_{s,cr}$ decreased with increasing size parameter according to the power-law

$$N_{s,cr} = K\chi_s^p \tag{12}$$

where K and p are empirical constants found, by least square fitting, to be $K = 136$ and $p = -0.7$ with a coefficient of determination $R^2 = 0.997$.

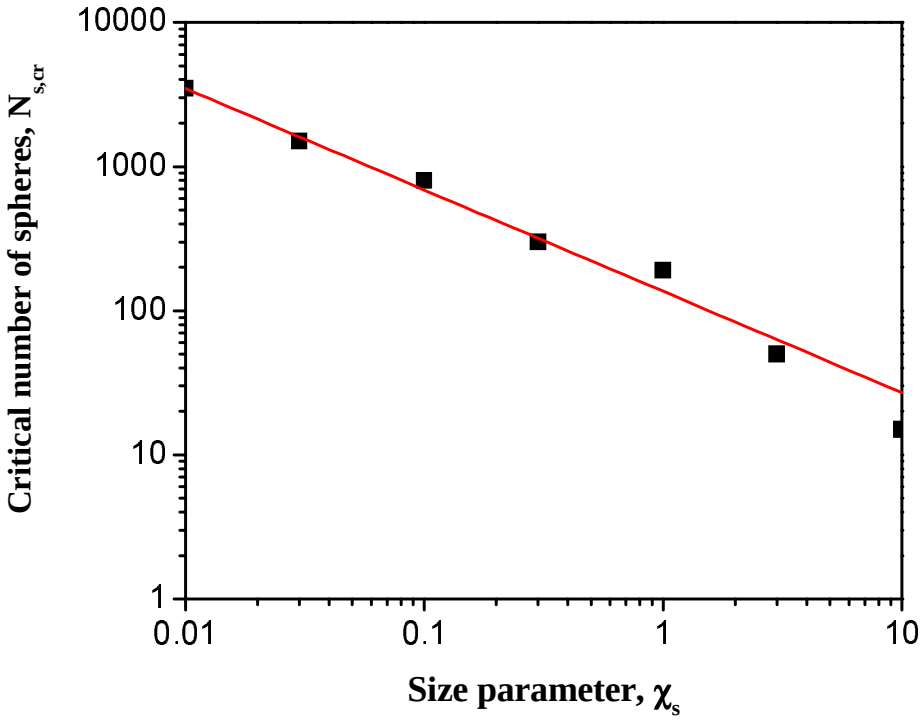

Figure 5: Critical number of spheres $N_{s,cr}$ beyond which the scattering cross-section $\langle C'_{sca} \rangle (m, \chi_s)$ of randomly oriented linear chains of spheres can be approximated as that of randomly oriented and infinitely long volume-equivalent cylinder as a function of size parameter χ_s.

4.2 Scattering Phase Function

Figure 6 shows the scattering phase function $F_{11}(\Theta)$ as a function of scattering angle Θ for randomly oriented linear chains of spheres consisting of $N_{s,cr}$ spheres with size parameter χ_s ranging between 0.01 and 10. It also shows the phase function for the corresponding randomly oriented and infinitely long volume-equivalent cylinders. The value of $F_{11}(0^o)$ for linear chains of spheres increased from 31.54 to 721.8 as the size parameter χ_s increased from 0.01 to 10. In other words, a linear chain of spheres scatter more and more strongly in the forward direction as the size parameter associated with individual constitutive spheres χ_s increases. Moreover, the scattering phase function of randomly oriented linear chain of sphere and infinitely long cylinders were very similar except in the forward and backward directions $\Theta = 0^o$ and 180^o. In addition, the scattering phase function shows strong oscillations for scattering angles larger than 20^o for χ_s=10. This indicates that resonance effects become increasingly important for large sphere size parameters.

Table 1 compares $F_{11}(0^o)$ and the asymmetry factors g_s and $g_{c,eq,V}$ for a long ($N_s = N_{s,cr}$) randomly oriented linear chain of spheres with that for a volume-equivalent cylinder. It indicates that the value of $F_{11}(0^o)$ for linear chains of spheres and infinitely long cylinders were significantly different. However, g_s and $g_{c,eq,V}$ differed by less than 1% and increased from 0.383 to 0.980 as χ_s increased from 0.01 to 10.

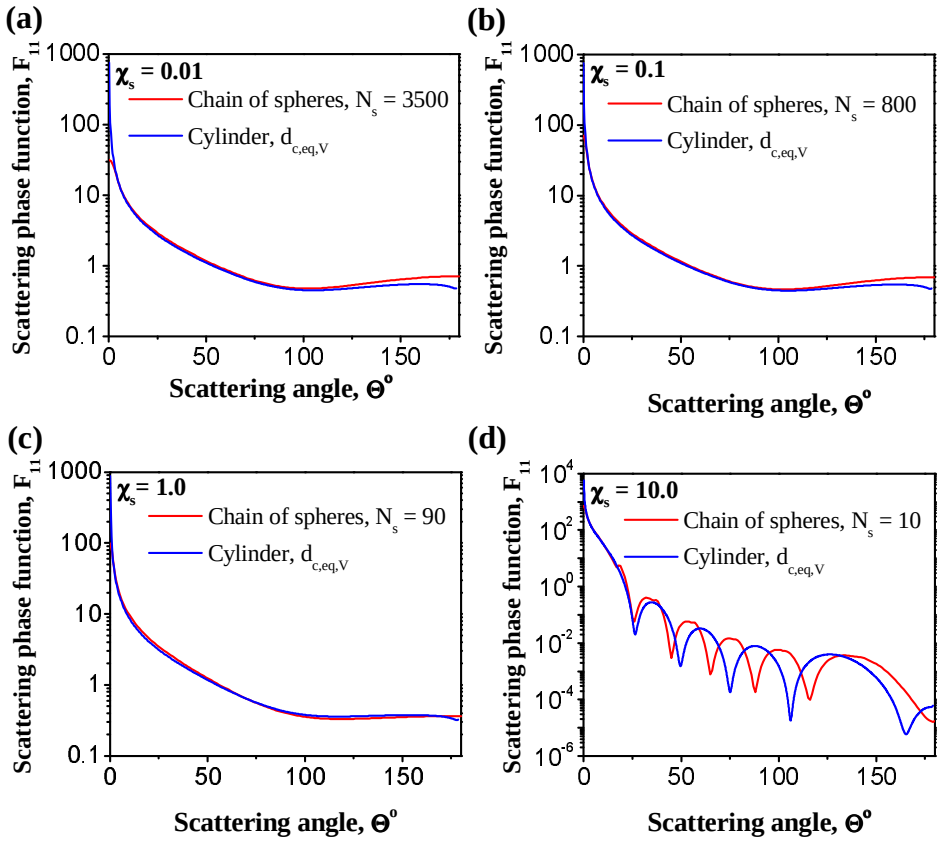

Figure 6: Scattering phase functions $F_{11}(\Theta)$ of randomly oriented long linear chains consisting of $N_{s,cr}$ monodisperse spheres or diameter d_s and randomly oriented and infinitely long volume-equivalent cylinders of diameter $d_{c,eq,V}$ as a function of scattering angle for χ_s=0.01, 0.1, 1.0, and 10.0 and $m = 1.0165 + i0.003$.

Table 1: Comparison between selected scattering properties of randomly oriented long linear chains of spheres with size parameter χ_s equals to 0.01, 0.1, 1.0, and 10.0 and their randomly oriented and infinitely long volume-equivalent cylinders. Their relative complex index of refraction was $m = 1.0165 + i0.003$.

Linear chain of spheres							Volume-equivalent cylinder				
χ_s	N_s	$\langle C'_{sca,s} \rangle$ (m)	$F_{11}(0^o)$	g_s	$\delta_{L,s}$	$\delta_{C,s}$	$\langle C'_{sca,s} \rangle$ (m)	$F_{11}(0^o)$	$g_{c,eq,V}$	$\delta_{L,c}$	$\delta_{C,c}$
0.01	4000	8.72×10^{-12}	37.3	0.38	0.0	0.0	9.098×10^{-12}	747.4	0.39	0.0	0.0
0.1	1300	8.87×10^{-8}	90.2	0.39	5.0×10^{-5}	8.0×10^{-17}	9.08×10^{-8}	748.7	0.39	0.0	0.0
1.0	190	7.26×10^{-4}	98.8	0.54	5.0×10^{-5}	7.6×10^{-17}	7.64×10^{-4}	878.3	0.49	0.0	0.0
10.0	15	1.085	721.8	0.98	0.09	0.2	1.086	5723.3	0.98	0.0	0.0

Overall, the above results establish that the radiation characteristics for unpolarized radiation of long (i.e., $N_s \geq N_{s,cr}$) randomly oriented linear chains of monodisperse spheres can be approximated as those of randomly oriented and infinitely long volume-equivalent cylinders. Then, their radiation characteristics can be computed using simple algorithm [1] instead of the superposition T-matrix method [21]. This simplifies and reduces significantly the computational effort.

For the practical problem of interest, filamentous cyanobacteria typically have size parameters larger than 10 and consist of more than 15 cells. Thus, the present study established that, as a first order approximation, filamentous cyanobacteria in photobioreactors can be approximated as randomly oriented and infinitely long cylinders for the purpose of predicting their radiation characteristics for unpolarized incident radiation.

4.3 Scattering Matrix Elements

In cases concerned with polarized radiation, for the purpose of remote sensing for example, detailed analysis of the Stokes scattering matrix element is necessary.

Figure 7 shows the ratios of the elements of the Stokes scattering matrix (a) -$F_{12}(\Theta)/F_{11}(\Theta)$, (b) $F_{22}(\Theta)/F_{11}(\Theta)$, (c) $F_{33}(\Theta)/F_{11}(\Theta)$, (d) $F_{44}(\Theta)/F_{11}(\Theta)$, and (e) $F_{34}(\Theta)/F_{11}(\Theta)$ as a function of scattering angle Θ for long ($N_s = N_{s,cr}$) randomly oriented linear chain of spheres of diameter d_s with size parameter χ_s equals to 0.01, 0.1, 1, and 10. It also shows these ratios for the corresponding randomly oriented and infinitely long cylinders with volume-equivalent diameter $d_{c,eq,V} = \sqrt{2/3}d_s$.

First, we observed that $\Delta(0^o)$ was equal to zero and that $F_{44}(180^o) = F_{11}(180^o) - 2F_{22}(180^o)$ for both long linear chains of spheres and infinitely long cylinders. We also verified that the results satisfied the symmetry relations for the scattering matrix elements of clusters of particles with one plane of symmetry expressed as [33]: $F_{12}(0^o) = F_{12}(180^o) = F_{34}(0^o) = F_{34}(180^o) = 0$, $F_{22}(0^o) = F_{33}(0)$, $F_{22}(180^o) = -F_{33}(180^o)$, $F_{11}(180^o) - F_{22}(180^o) = F_{44}(180^o) - F_{33}(180^o)$, and $F_{11}(180^o) - F_{22}(180^o) = F_{44}(180^o) - F_{33}(180^o)$.

Second, it is worth noting that the ratios of the elements of the Stokes scattering matrix for long linear chains of monodisperse spheres were nearly identical to one another for size parameter χ_s between 0.01 and 1. The behavior of the matrix element ratios were very similar to results reported (i) by Liu and Mishchenko [35] for orientation-averaged scattering matrix elements of fractal-like soot aggregates consisting of more than 200 monodisperse spherical monomers of diameter $d_s = 20$ nm with $m = 1.75 + 0.435$ at λ=628 nm ($\chi_s = 0.1$), and (ii) by Bunkin *et al.* [47] for ensemble-averaged scattering matrix elements of stochastic ensembles of non-absorbing nanosphere clusters made of 500 $\pm$ 70 polydisperse monomers with mean diameter of 100 nm and $m = 0.75$ at λ=532 nm ($\chi_s \sim 0.6$).

Moreover, for a given value of χ_s, increasing the numbers of spheres in the linear chain significantly affected the scattering phase function $F_{11}(\Theta)$ but not the ratios $F_{12}(\Theta)/F_{11}(\Theta)$, $F_{22}(\Theta)/F_{11}(\Theta)$, $F_{33}(\Theta)/F_{11}(\Theta)$, $F_{44}(\Theta)/F_{11}(\Theta)$, and $F_{34}(\Theta)/F_{11}(\Theta)$. This was also observed for linear chains of spheres with large size parameter ($\chi_s = 5$) [19] and for fractal-like soot aggregates [35].

The degree of linear polarization of linear chains of spheres for unpolarized incident radiation $-F_{12}(\Theta)/F_{11}(\Theta)$ reached a maximum of 100% at scattering angle Θ around 90^o. It also vanished in the forward scattering ($\Theta = 0^o$) and backscattering angles ($\Theta = 180^o$),

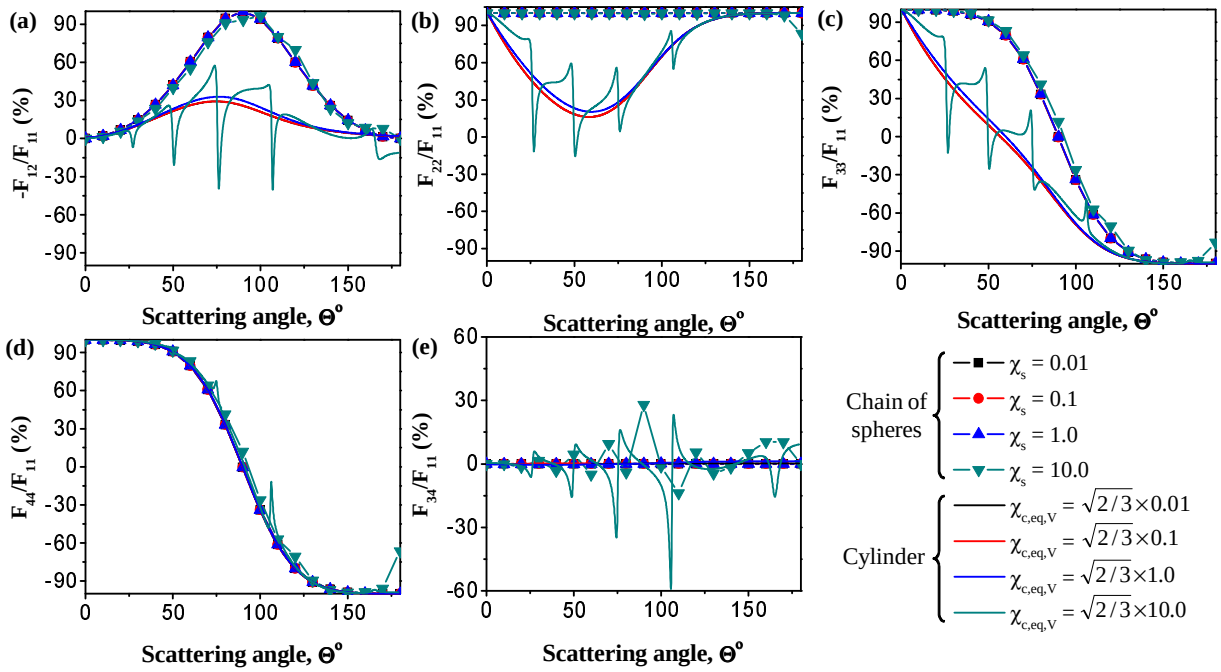

Figure 7: Scattering matrix element ratios (a) $-F_{12}(\Theta)/F_{11}(\Theta)$, (b) $F_{22}(\Theta)/F_{11}(\Theta)$, (c) $F_{33}(\Theta)/F_{11}(\Theta)$, and (d) $F_{44}(\Theta)/F_{11}(\Theta)$ as a function of scattering angle Θ for randomly oriented linear chains of spheres consisting of $N_{s,cr}$ monodisperse spheres of diameter d_s and of infinitely long cylinders of volume-equivalent diameter as function of scattering angle for χ_s=0.01, 0.1, 1.0, and 10 and $m = 1.0165 + i0.003$.

as expected for a cluster of spheres with a plane of symmetry [19, 48]. Similar results were obtained for a fractal cluster of soot particles and were attributed to the fact that scattering was dominated by individual Rayleigh-sized spheres [22, 35]. In addition, the light scattered by multiple spheres was more linearly polarized than that by the volume-equivalent cylinder. In fact, $-F_{12}(\Theta)/F_{11}(\Theta)$ reached a maximum of about 30-35% around 80^o for randomly oriented and infinitely long volume-equivalent cylinders and was nearly independent of χ_s except for $\chi_s = 10$. In this latter case, $-F_{12}(\Theta)/F_{11}(\Theta)$ featured resonances at the same scattering angles as those observed in $F_{11}(\Theta)$.

The ratio $F_{22}(\Theta)/F_{11}(\Theta)$ was equal to 100% at all scattering angles for randomly oriented linear chains of spheres for any size parameters. These results were identical to those obtained with a single sphere and further confirm the above observations the single spheres dominated scattering. However, the linear and circular polarization ratios $\delta_{L,s}$ and $\delta_{C,s}$ were nearly 0.0 for $\chi_s \leq 1$ and increased for larger size parameters χ_s. Unlike single spheres, $\delta_{L,s}$ and $\delta_{C,s}$ were different for all size parameters, as summarized in Table 1. For an infinitely long cylinders, $F_{22}(\Theta)/F_{11}(\Theta)$ was 100% for forward ($\Theta = 0^o$) and backward ($\Theta = 180^o$) scattering angles but decreased between these two angles reaching a minimum of about 20% for scattering angle around 50^o. As previously mentioned, $\delta_{C,c}$=$\delta_{C,c}$=0 for randomly oriented and infinitely long cylinders of any size parameter.

For both randomly oriented cylinders and linear chains of spheres, the ratios $F_{33}(\Theta)/F_{11}(\Theta)$

and $F_{44}(\Theta)/F_{11}(\Theta)$ decreased from 100% to -100% as the scattering angle increased from 0 to 180^o. The ratio $F_{33}(\Theta)/F_{11}(\Theta)$ decreased faster for a cylinder than for a linear chain of spheres. However, the ratio $F_{44}(\Theta)/F_{11}(\Theta)$ was nearly identical for randomly oriented linear chains of aligned spheres and infinitely long cylinders with volume-equivalent diameter for all size parameter χ_s considered. The ratios $F_{33}(\Theta)/F_{11}(\Theta)$ and $F_{44}(\Theta)/F_{11}(\Theta)$ for long linear chains of spheres were equal to each other and were identical to those of a single sphere. This was unlike what was observed in the validation cases for bispheres [18] and for linear chains of 1-5 spheres [19] with size parameter of 10 and 5, respectively. Indeed, in these cases, the ratio $F_{22}(\Theta)/F_{11}(\Theta)$ departed from unity and the ratio $F_{33}(\Theta)/F_{11}(\Theta)$ was different from $F_{44}(\Theta)/F_{11}(\Theta)$, unlike those corresponding to a single sphere.

Finally, the Stokes scattering matrix element ratio $F_{34}(\Theta)/F_{11}(\Theta)$ was equal to 0.0 for all scattering angles for χ_s= 0.01, 0.1, and 1 for both randomly oriented linear chains of spheres and infinitely long cylinders. However, for $\chi_s = 10$, $F_{34}(\Theta)/F_{11}(\Theta)$ featured several peaks with values between -60% and 30% at scattering angles corresponding to the resonances observed in $F_{11}(\Theta)$ as well as in the other scattering element ratios. These resonance angles and the associated value of $F_{34}(\Theta)/F_{11}(\Theta)$ were significantly different from those for volume-equivalent infinitely long cylinder.

Overall, the volume-equivalent cylinder featured Stokes scattering element matrix ratios very different from those linear chains of spheres. The equivalence observed for the absorption and scattering cross-sections per unit length and for the asymmetric factor do not apply to the Stokes scattering matrix element ratios other than $F_{44}(\Theta)/F_{11}(\Theta)$.

4.4 Effects of Polydispersity

The radiation characteristics of linear chains of spheres can be affected by the spheres' polydispersity. To assess this effect in the context of filamentous cyanobacteria shown in Figure 1, we considered two different linear chains of fourteen spheres with average diameter $\bar{d}_s$ of 3.323 μm and 3.753 μm and standard deviation σ equals to 0.952 μm and 0.468 μm, respectively. The smallest and largest spheres were 2.617 and 4.655 μm in diameter for a size parameter ranging between 6 and 10. The size distributions of the two chains were representative of those measured for cyanobacterium *Anaebena cylindrica*. Here also, the complex index of refraction was $m = 1.0165 + i0.003$ for all spheres.

Table 2 compares the absorption and scattering cross-sections of the above-described randomly oriented linear chains of polydisperse spheres and those of the linear chain of monodisperse spheres with the corresponding average diameter $\bar{d}_s$. The results indicate that the cross-sections $\langle C'_{abs,s}\rangle$ and $\langle C'_{sca,s}\rangle$ for Chain 1 fell within 10% of those of a chain with monodisperse spheres of average diameter $\bar{d}_s$. The differences in $\langle C'_{abs,s}\rangle$ and $\langle C'_{sca,s}\rangle$ fell within 2% for Chain 2. This can be attributed to the narrower size distribution of Chain 2 compared with Chain 1. Overall, these results suggest that for the polydispersity typically encountered in vegetative cells and heterocysts, the cells in the filaments can be treated as monodisperse with the average cell diameter for estimating the absorption and scattering cross-sections.

Table 2: Comparison of the absorption and scattering cross-sections $\langle C_{abs,s} \rangle$ and $\langle C_{sca,s} \rangle$ of two randomly oriented linear chains of spheres (a) with representative arbitrary diameter distribution and (b) with monodisperse spheres with the corresponding average diameter $\bar{d}_s$. The complex index of refraction was $m = 1.0165 + i0.003$ for all spheres.

	Polydisperse spheres				Monodisperse spheres		
Chain #	d_s (μm)	σ (μm)	$\langle C'_{abs,s} \rangle$ (m^2)	$\langle C'_{sca,s} \rangle$ (m^2/m)	d_s (μm)	$\langle C'_{abs,s} \rangle$ (m^2)	$\langle C'_{sca,s} \rangle$ (m^2/m)
1	2.62-4.65	0.48	0.136	0.179	3.32	0.122	0.170
2	3.31-4.14	0.23	0.178	0.218	3.75	0.174	0.215

5 CONCLUSION

This study presented predictions of the radiation characteristics and Stokes scattering matrix elements of linear chains of monodisperse spheres. The results established that scattering and absorption cross-sections per unit length of randomly oriented linear chains of monodisperse spheres and their asymmetry factor can be approximated as those of randomly oriented and infinitely long cylinders with volume-equivalent diameter provided that the number of spheres is larger than the critical sphere number $N_{s,cr} = 136\chi_s^{0.7}$. Finally, approximating long linear chains of spheres with infinitely long cylinders does not extend to the Stokes scattering matrix element ratios. These results can be used in retrieving the optical properties of filamentous cyanobacteria from experimental measurements absorption and scattering cross-sections.

References

[1] M. Kerker, *The Scattering of Light, and Other Electromagnetic Radiation* (Academic Press, New York, NY, 1969).

[2] C. Bohren and D. Huffman, *Absorption and Scattering of Light by Small Particles* (John Wiley & Sons, New York, NY, 1998).

[3] K. Liou, *An Introduction to Atmospheric Radiation* (Academic Press, San Diego, CA, 2002), 2nd ed.

[4] M. Jonasz and G. Fournier, *Light Sscattering by Particles in Water: Theoretical and Experimental Foundations* (Academic Press, San Diego, CA, 2007).

[5] M. Mishchenko and L. Travis, "Light scattering by polydispersions of randomly oriented spheroids with sizes comparable to wavelengths to observation," *Applied Optics* **33**, 7206–7225 (1994).

[6] M. I. Mishchenko and J. W. Hovenier, "Depolarization of light backscattered by randomly oriented nonspherical particles," *Optics Letters* **20**, 1356–1358 (1995).

[7] M. Mishchenko, L. Travis, and D. Mackowski, "T-matrix computations of light scattering by nonspherical particles: A review," *Journal of Quantitative Spectroscopy and Radiative Transfer* **55**, 535 – 575 (1996).

[8] M. Mishchenko, J. Hovenier, and L. Travis, *Light Scattering by Nonspherical Particles* (Academic Press, San Diego, CA, 2000).

[9] D. Mackowski, "Discrete dipole moment method for calculation of the T matrix for nonspherical particles," *Journal of the Optical Society of America A* **19**, 881–893 (2002).

[10] E. Purcell and C. Pennypacker, "Scattering and absorption of light by nonspherical dielectric grains," *Astrophysical Journal* **186**, 705–714 (1973).

[11] B. Draine, "The discrete-dipole approximation and its application to interstellar graphite grains," *Astrophysical Journal* **333**, 848–872 (1988).

[12] B. Draine and P. Flatau, "Discrete-dipole approximation for scattering calculations," *Journal of the Optical Society of America A* **11**, 1491–1499 (1994).

[13] P. Yang and K. Liou, "Finite-difference time domain method for light scattering by small ice crystals in three-dimensional space," *Journal of the Optical Society of America A* **13**, 2072–2085 (1996).

[14] P. Yang, G. Kattawar, and W. Wiscombe, "Effect of particle asphericity on single-scattering parameters: Comparison between platonic solids and spheres," *Applied Optics* **43**, 4427–4435 (2004).

[15] M. Mishchenko and D. Mackowski, "Light scattering by randomly oriented bispheres," *Optics Letters* **19**, 1604–1606 (1994).

[16] D. Mackowski, "Calculation of total cross sections of multiple-sphere clusters," *Journal of the Optical Society of America A* **11**, 2851–2861 (1994).

[17] M. Mishchenko, D. Mackowski, and L. Travis, "Scattering of light by bispheres with touching and separated components," *Applied Optics* **34**, 4589–4599 (1995).

[18] M. Mishchenko and D. Mackowski, "Electromagnetic scattering by randomly oriented bispheres: Comparison of theory and experiment and benchmark calculations," *Journal of Quantitative Spectroscopy and Radiative Transfer* **55**, 683 – 694 (1996).

[19] D. Mackowski and M. Mishchenko, "Calculation of the T matrix and the scattering matrix for ensembles of spheres," *Journal of the Optical Society of America A* **13**, 2266–2278 (1996).

[20] D. Mackowski, "A simplified model to predict the effects of aggregation on the absorption properties of soot particles," *Journal of Quantitative Spectroscopy and Radiative Transfer* **100**, 237 – 249 (2006).

[21] D. Mackowski and M. Mishchenko, "A multiple sphere T-matrix Fortran code for use on parallel computer clusters," *Journal of Quantitative Spectroscopy and Radiative Transfer* **112**, 2182–2192 (2011).

[22] R. West, "Optical properties of aggregate particles whose outer diameter is comparable to the wavelength," *Applied Optics* **30**, 5316–5324 (1991).

[23] M. Iskander, H. Chen, and J. Penner, "Optical scattering and absorption by branched chains of aerosols," *Applied Optics* **28**, 3083–3091 (1989).

[24] M. Iskander, H. Chen, and J. Penner, "Resonance optical absorption by fractal agglomerates of smoke aerosols," *Atmospheric Environment. Part A. General Topics* **25**, 2563 – 2569 (1991).

[25] S. Manickavasagam and M. P. Mengüç, "Scattering matrix elements of fractal-like soot agglomerates," *Applied Optics* **36**, 1337–1351 (1997).

[26] F. Kahnert, J. Stamnes, and K. Stamnes, "Can simple particle shapes be used to model scalar optical properties of an ensemble of wavelength-sized particles with complex shapes?" *Journal of the Optical Society of America A* **19**, 521–531 (2002).

[27] M. Madigan and J. Martinko, *Biology of Microorganisms* (Pearson Prentice Hall, Upper Saddle River, NJ, 2006).

[28] L. Stal, "Cyanobacteria," in "Algae and Cyanobacteria in Extreme Environments," , vol. 11 of *Cellular Origin, Life in Extreme Habitats and Astrobiology*, J. Seckbach, ed. (Springer, Netherlands, 2007), pp. 659–680.

[29] J. Benemann, "Hydrogen production by microalgae," *Journal of Applied Phycology* **12**, 291–300 (2000).

[30] M. Mishchenko, L. Travis, and A. Lacis, *Scattering, Absorption, and Emission of Light by Small Particles* (Cambridge University Press, Cambridge, UK, 2001).

[31] L. Pilon, H. Berberoğlu, and R. Kandilian, "Radiation transfer in photobiological carbon dioxide fixation and fuel production by microalgae," *Journal of Quantitative Spectroscopy and Radiative Transfer* **112**, 2639 – 2660 (2011).

[32] S. Manickavasagam and M. Mengüc, "Scattering-matrix elements of coated infinite-length cylinders," *Applied Optics* **37**, 2473–2482 (1998).

[33] J. Hovenier and D. Mackowski, "Symmetry relations for forward and backward scattering by randomly oriented particles," *Journal of Quantitative Spectroscopy and Radiative Transfer* **60**, 483 – 492 (1998).

[34] S. Lee, "Radiative transfer through a fibrous medium: Allowance for fiber orientation," *Journal of Quantitative Spectroscopy and Radiative Transfer* **36**, 253–263 (1986).

[35] L. Liu and M. Mishchenko, "Effects of aggregation on scattering and radiative properties of soot aerosols," *Journal of Geophysical Research: Atmospheres* **110** (2005).

[36] A. Lind and J. Greenberg, "Electromagnetic scattering by obliquely oriented cylinders," *Journal of Applied Physics* **37**, 3195–3203 (1966).

[37] T. Tong and C. Tien, "Analytical models for thermal radiation in fibrous insulations," *Journal of Building Physics* **4**, 27–44 (1980).

[38] S. Lee, "Radiation heat-transfer model for fibers oriented parallel to diffuse boundaries," *Journal of Thermophysics and Heat Transfer* **2**, 303–308 (1988).

[39] H. Yousif and E. Boutros, "A FORTRAN code for the scattering of EM plane waves by an infinitely long cylinder at oblique incidence," *Computer Physics Communications* **69**, 406 – 414 (1992).

[40] M. Modest, *Radiative Heat Transfer* (Academic Press, San Diego, CA, 2003).

[41] Z.-J. Li, Z.-S. Wu, Y. Shi, L. Bai, and H.-Y. Li, "Multiple scattering of electromagnetic waves by an aggregate of uniaxial anisotropic spheres," *Journal of the Optical Society of America A* **29**, 22–31 (2012).

[42] D. Stramski, A. Bricaud, and A. Morel, "Modeling the inherent optical properties of the ocean based on the detailed composition of planktonic community," *Applied Optics* **40**, 2929–2945 (2001).

[43] J.-F. Cornet, C. Dussap, J. Gross, C. Binois, and C. Lasseur, "A simplified monodimensional approach for modeling coupling between radiant light transfer and growth kinetics in photobioreactors," *Chemical Engineering Science* **50**, 1489–1500 (1995).

[44] J. Cornet and C. Dussap, "A simple and reliable formula for assessment of maximum volumetric productivities in photobioreactors," *Biotechnology Progress* **25**, 424–435 (2009).

[45] E. Lee, R.-L. Heng, and L. Pilon, "Spectral optical properties of selected photosynthetic microalgae producing biofuels," *Journal of Quantitative Spectroscopy and Radiative Transfer* **114**, 122 – 135 (2013).

[46] S.C.Lee, "Scattering phase function for fibrous media," *International Journal of Heat and Mass Transfer* **33**, 2183–2190 (1990).

[47] N. Bunkin, A. Shkirin, N. Suyazov, and A. Starosvetskiy, "Calculations of light scattering matrices for stochastic ensembles of nanosphere clusters," *Journal of Quantitative Spectroscopy and Radiative Transfer* **123**, 23 – 29 (2013).

[48] J. Hovenier, H. van de Hulst, and C. van der Mee, "Conditions for the elements of the scattering matrix," *Astronomy and Astrophysics* **157**, 301–310 (1986).